Tailoring Soft Local Zones in Quenched Blanks of the Steel 22MnB5 by Partial Pre-cooling with Compressed Air

Oleksandr Golovko, Max-Henry Stolte, Kai Wölki, Sven Hübner, Bernd-Arno Behrens, Hans Jürgen Maier, and Florian Nürnberger

The high-strength boron steel 22MnB5 steel is widely used for automotive lightweight constructions. A novel approach is promising to tailor strength and ductility in the hardened condition using locally pre-tempered sheets for the hot stamping process. It results in the formation of locally soft spots where mechanical joining is subsequently intended. A slow pre-cooling of the later joining zones with cooling rates below a certain critical cooling rate for obtaining a decreased strength in these regions is required. A tubular air cooling system suited for this task is presented and tested in a process where the subsequent quenching of the overall sheet is realized by rapid cooling in a water bath. Varying the air pressure and cooling duration allows controlling the size of the softened local spot in a wide range and still obtaining a bainitic microstructure. Using two-stage cooling with point jet nozzles and a subsequent hot stamping process with water-cooled dies resulted in a main sheet hardness of about 470 HV5 and of 260 HV5 in the pre-cooled spots, respectively.

1. Introduction

High-strength steels are of great interest for automotive lightweight constructions as these allow employing sheets with reduced thickness (Ref 1–3). A further efficiency increase can be realized by the application of tailored tempering (Ref 4–6). In this concept, high-strength sections are combined with ductile sections in one single structural part. Hence, such parts feature both sections suited for mechanical joining operations as well as high-strength areas needed to improve the safety of the vehicles. In the same context, material zones with a locally reduced strength and increased ductility can be used to increase the energy absorption capacity and thus crash performance (Ref 7–11).

Several technologies are available to obtain tailored properties in combination with hot stamping (cf. Table 1):

- One approach uses partial heating limited to certain sections of the blanks prior to the hot stamping. The later soft zones have to be kept below the Ac_1-temperature in order to prevent microstructural transformations into austenite and retain the initial soft ferritic-perlitic microstructure (Ref 12–14). In contrast, the sections that are to be hardened have to be heated above the Ac_3-temperature in order to generate a fully martensitic microstructure during the quenching while hot stamping with water-cooled tools. For such routes, furnaces with different independently controlled heating zones are required featuring a ceramic brick insulation between each heating zone (Ref 15). One disadvantage of this method is high energy expenses (Ref 16). Furthermore, it is possible to use alternative heating processes that ensure high heating rates and low oxidation, such as inductive (Ref 17, 18), conductive (Ref 18, 19) and contact (Ref 20, 21) heating. However, these might be disadvantageous due to extensive equipment, non-uniformity of heating or the necessity to use uncoated sheets.

- Partial properties after press hardening can be realized using tailored pre-cooling in a multizone tempering station after heating in common roller heard furnace (Ref 22, 23). The tempering station holds a section of the blank in the austenitized state before press hardening using burners as well as induction, conduction or contact heating. Other sections of the blank are cooled to obtain a bainitic structure. A novel variation of such approach is developed in the present work.

- Common alternative approaches apply differing cooling conditions to homogenously austenitized blanks during hot stamping. Examples are partially heated tools, tools with sections of differing thermal properties or the die relief method (Ref 1, 16, 24, 25). In all cases a complex tool design results.

- The application of differing cooling conditions using early extraction in a hot stamping process was proposed in Die-

Oleksandr Golovko, Max-Henry Stolte, Hans Jürgen Maier, and **Florian Nürnberger**, Institut für Werkstoffkunde (Materials Science), Leibniz Universität Hannover, An der Universität 2, 30823 Garbsen, Germany; and **Kai Wölki, Sven Hübner,** and **Bernd-Arno Behrens**, Institut für Umformtechnik und Umformmaschinen (Institute of Forming Technology and Machines), Leibniz Universität Hannover, An der Universität 2, 30823 Garbsen, Germany. Contact e-mails: golovko@iw.uni-hannover.de, stolte@iw.uni-hannover.de, woelki@ifum.uni-hannover.de, huebner@ifum.uni-hannover.de, behrens@ifum.uni-hannover.de, maier@iw.uni-hannover.de, and nuernberger@iw.uni-hannover.de.

Table 1 Technologies for tailoring properties locally in hot stamping processes

#	Approach	Process classification	Technology	Effect	Advantages	Disadvantages	References
I	Partial austenitizing of blanks	Prior to hot stamping	Ceramic insulation in a common furnace between different blank zones	Only fully austenitized material sections will be hardened during hot stamping by martensitic transformation	Conventional hot stamping tools can be used	Furnace with independent heating zones required; High energy demand	(Ref 5, 12–16)
			Inductive heating		High heating rate and low oxidation; Usage of uncoated sheets	High complexity of equipment	(Ref 1, 17–19)
			Conductive heating			Non uniform heating of a main blank	
			Contact heating		Blank surface is isolated during heating preventing oxidation	Difficulty in achieving small areas with lowered temperature	(Ref 20, 21)
IIa	Full austenitizing of blanks with subsequent local pre-cooling	Prior to hot stamping	Multizoned tempering device (inductive, conductive, and contact)	Pre-cooled local zones transform to softer bainite prior to hot stamping due to activation of diffusional processes	Conventional furnaces and hot stamping tools can be used	Additional process step; Necessity of individual tools for different part geometries	(22, 23)
IIb			Local pressurized air or spray cooling		Universal applicability for different structural element geometries	External pre-cooling with locally adaptable air pressures required	*
IIIa	Locally different cooling rate of parts	During hot stamping	Partially heated tools	Differing die temperatures result in high/low cooling rates and hence martensitic (hard) and bainitic (softer) sections, respectively	Fully austenitized blanks applicable	Complex and costly die design; Long hot stamping processing times	(Ref 1, 16, 22, 24, 25)
IIIb			Tools with differing thermal properties	Differing heat conductivity results in high/low cooling rates and hence both martensitic (hard) and bainitic (softer) sections		Complex die design; Costly tool materials; Long hot stamping processing times	
IIIc			Die relief method	Differing contact pressure or die-to-blank distance results in high/low cooling rates and hence martensitic (hard) and bainitic (softer) sections, respectively		Complex process design; Long hot stamping processing times	

Table 1 continued

#	Approach	Process classification	Technology	Effect	Advantages	Disadvantages	References
IIId		Early extraction during hot stamping	Local pressurized air or spray cooling	Differing heat transfer coefficients result in high/low cooling rates and hence martensitic (hard) and bainitic (softer) sections, respectively	Fully austenitized blanks and conventional hot stamping tools can be used Short hot stamping processing times	External cooling with locally adaptable air or water-spray pressures required Increased potential for distortion	(Ref 26, 27)
IV	Partial tempering of the fully hardened parts	After hot stamping	Local—e. g. inductive -heating after quenching	Local tempering to soften the martensite	Fully austenitized blanks and conventional hot stamping tools can be used	Additional process step and heating tools required after hot stamping	(Ref 22, 28)

kamp et al. (Ref 26, 27). In this approach of partial quenching, blanks are fully austenitized in a furnace, hot stamped with a reduced holding time of only 0.6 s and subsequently locally cooled with a water-air spray. Due to the locally adapted heat transfer conditions, hardened martensitic sections as well as softer bainitic ones can be achieved. Suited extraction temperature of the parts from the hot stamping press was in the range of 450–530 °C. Cooling rates of about 64 K/s in hard zones and 2 K/s in soft zones allowed to realize a Vickers hardness difference up to 200 HV10.

- Alternatively, a partially tempering of the fully hardened parts after hot stamping can be applied though this requires an additional subsequent processing step (Ref 28).

Since these technologies rely either on a complex furnace design, long processing times during hot stamping or further additional subsequent processing steps, alternative approaches are of significant interest. In the present study, local pre-cooling of fully austenitized blanks prior to the hot stamping was employed, since conventional furnaces and heating strategies for the full austenitization can be applied and no modifications of the hot stamping tools are required. In the proposed approach (cf. Table 1, approach II), sections of reduced hardness are realized by local pre-cooling to intermediate temperatures prior to the hot stamping to allow diffusional processes to take place, and thus prematurely form bainite instead of martensite during the actual hot stamping (s. Fig. 1). Compared to approach IIId (cf. Table 1), a negligible residual distortion of the hot stamped parts can be expected. Using the example of the boron-alloyed steel 22MnB5 (1.5528), the intention was to realize softened sections with a large difference in hardness as compared to the martensitic matrix. Compressed air was used to pre-cool these sections prior to the hot stamping and thus promote a bainitic transformation. In order to reduce the experimental effort, the final cooling of the blanks was carried out by water quenching in most of the experiments. For selected cases, an industrial press with a water-cooled tool was employed in order to evaluate the transfer potential of the proposed approach with respect to actual application.

2. Material Properties

The boron-alloyed steel 22MnB5 (1.5528) was used in the form of blanks with a sheet thickness of 1.5 mm. The actual chemical composition is provided in Table 2 and was determined using an optical emission spectrometer (SPECTRO-MAXx LMX06). In order to prevent scaling due to high-temperature oxidation in the furnace and provide a protection against corrosion, the sheets are coated with an Al-Si layer, which obtains its final properties due to diffusional processes during heating and holding in the furnace.

The as-received sheets featured a ferritic-perlitic structure with mechanical properties summarized in Table 3. The dependence of the properties with respect to the direction relative to the rolling axis was found to be low with variations of no more than 2% for the strength characteristics and up to 3% for the ductility.
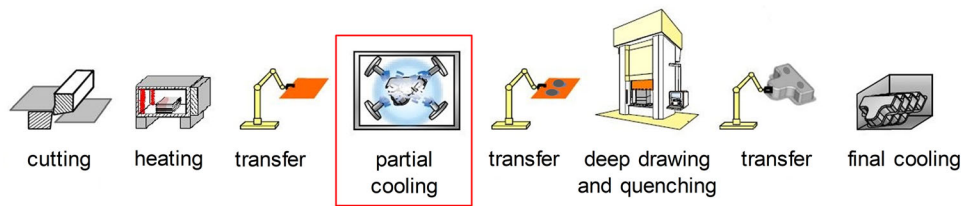
Fig. 1 Proposed process chain featuring a local pre-cooling prior to the hot stamping to create soft bainitic microstructures

Table 2 Nominal and measured chemical composition of the initial sheets, wt.%

Element	Fe	C	Si	Mn	P	S	Al	Cr	Ti	B
Nominal (29)	Bal.	0.19–0.25	≤ 0.40	1.1–1.4	≤ 0.0245	≤ 0.015	0.02–0.06	0.15–0.35	0.02–0.05	0.0008–0.005
Measured	97.88	0.233	0.268	1.18	0.011	0.002	0.038	0.18	0.031	0.0039

Table 3 Mechanical properties of blanks in the initial condition, measured using tensile samples according to DIN 50125—H 12.5 × 50

Direction	Ultimate tensile strength, MPa	0.2% offset yield stress, MPa	Total elongation at fracture, %
Lengthwise	611	386	22.3
Crosswise	619	394	22.1
45°	609	395	22.8

3. Methods

3.1 Layout of the Blank with Pre-cooled Sections

The sheets used featured a size of 200 mm × 260 mm. Softened sections were chosen to be separated 84 and 200 mm from each other. As marked in Fig. 2, the temperature-time profile was recorded at the four selected positions no. 1–4 during heating and at the positions no. 3 and 4 during cooling. Temperature was measured with Ni-NiCr thermocouples that were spot-welded to the blank surface.

3.2 Local Pre-cooling

The developed tubular cooling device for the local pre-cooling of the sheets by compressed air is depicted in Fig. 3. The cooling air is fed through an inner cooper tube with an inside diameter of 5 mm. A small point jet nozzle LU-VS201295-18, Fa. "Spraying Systems," was mounted optionally to the outlet of the inner tube. This nozzle is characterized with one central hole and six peripherally guiding holes. The air heated up by the hot sheet is exhausted through the outer tube (Fig. 3, left), which had an inside diameter of 16 mm. In order to minimize air leakage, a spring mounted foot cap was used at the bottom of each outer tube. The tube sets were arranged in a pneumatically driven rectangular frame with a thermally insulated plate at the bottom (steel covered with an insulating layer). An electrically heated stainless-steel plate, which is referred to as the "temperature control plate," is positioned at the bottom of the housing featuring a maximal possible temperature of 850 °C.
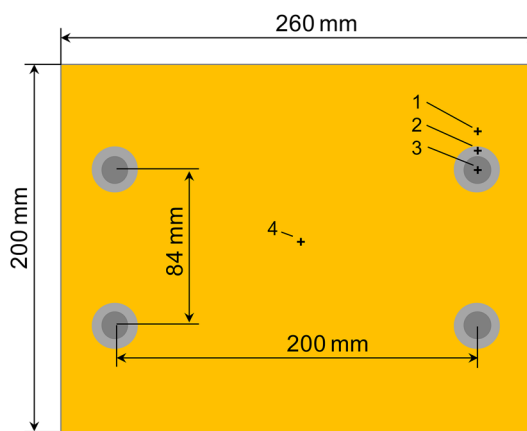

Fig. 2 Layout of softened sections on the processed blank (1: non-pre-cooled position close to a pre-cooling spot; 2: transition zone; 3: center of pre-cooled section; 4: non-pre-cooled position in the center of the sheet)

3.3 Austenitization Prior to Pre-cooling

In order to be fully austenitized, the steel 22MnB5 is normally exposed to a furnace temperature of 850–950 °C with a dwell time between 3 and 6 min (Ref 1, 30). In the present study, the furnace temperature was increased to 1050 °C in order to ensure a sheet temperature of 870–900 °C prior to quenching regarding a possible heat loss not only in the later pre-cooled sheet sections (desired) but in the non-pre-cooled areas as well (non-desired). Total time of heating and holding
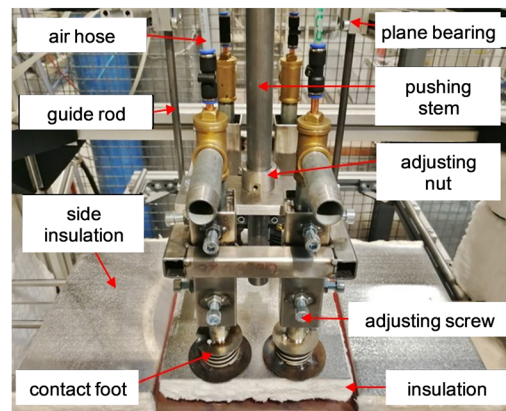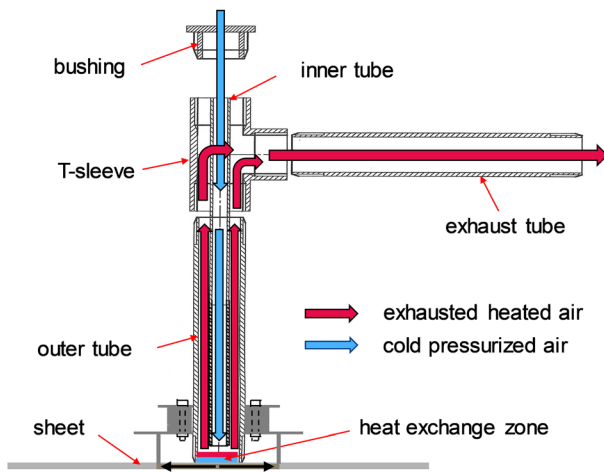
Fig. 3 Schematic showing the tubular cooling device (left) and actual setup (right)
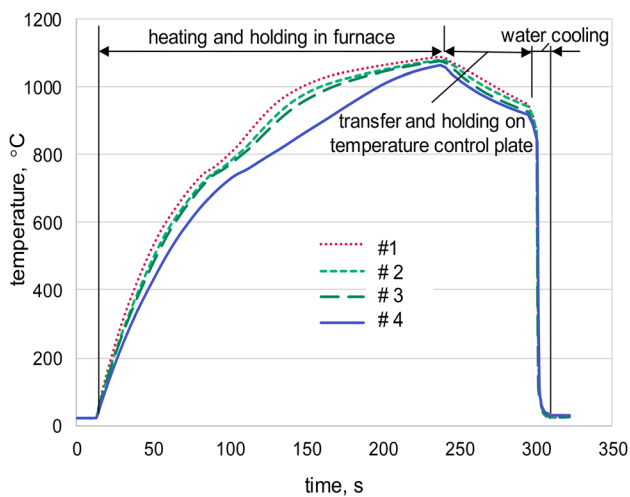

Fig. 4 Representative temperature-time profile at the control points (Pos. 1–4, cf. Fig. 2) during heating, transfer and final water quenching

was set to 4 min. The resulting temperature-time profiles for the selected control points are shown in Fig. 4.

3.4 Air-Cooling Conditions

To evaluate the characteristics of the pre-cooling by compressed air, furnace-heated sheets were transferred in a thermally insulated container to the temperature control plate, which was heated to 800 °C. Then, the frame with the tubular cooling devices was clamped to the hot sheets and the compressed air fed to the tubes for cooling. The distance of the outlet of the inner tube to the sheet surface was varied from 5 to 20 mm. In these experiments, the air pressure was varied from 0.1 to 0.4 MPa with a constant cooling time of 40 s. The air flow rate reached the nominal values within approx. 2 s. For this setup, the flow rate w in l/min depends linearly on the nominal air pressure p in MPa:

$$w = 23 + 353 \cdot p \qquad (Eq\ 1)$$

After pre-cooling with compressed air, the samples were transferred to the water bath within 3 s and quenched. Based on

the data from the experiments with pre-cooling for 40 s, cooling conditions were varied in an attempt to reduce the overall cooling time (cf. Table 4). Provided that the bainitic transformation can be activated quickly in a first cooling step, more rapid quenching can be applied in the second. In such a way, the total processing time can be shortened.

3.5 Microstructure Adapted Local Cooling Strategy

According to the proposed approach, the cooling of the samples was carried out in several stages. After furnace heating, the samples were slowly air cooled in one or two steps at the designated four positions with cooling rates of no more than the critical cooling rate of 27 K/s to prevent a premature transformation to martensite (Ref 1). At the end of this slow cooling, the temperature at the air-cooled points had to meet the one for the bainitic regime as given by the time–temperature–transformation diagram (cf. Fig. 5) with temperatures ranging from 400 to 600 °C. The cooling curve for the soft zones is schematically depicted by the line marked 1. At the same time, the material sample sections which are to be hardened by later quenching had to be held at a temperature above Ac_3 (line 2 in Fig. 5). In the final stage, the samples were rapidly cooled by water quenching so that the non-pre-cooled material sections transformed a fully martensitic microstructure.

The final experimental series of hot stamping was carried out using an industrial press (Dunkes HD250) with water cooled tools instead of water bath quenching as the last operation of processing. Total time of the hot stamping was 8 s.

3.6 Specimen Preparation and Characterization

After the experiments, two types of specimens were used to measure the Vickers hardness and to characterize the microstructure (44 mm × 15 mm) as well as to prepare tensile test specimen (12.5 mm × 30 mm). For the latter, the circular pre-cooled section was in the center of the gauge length. The Vickers hardness test was conducted with a force of 49 N (HV5). For every parameter combination, 5 specimens were tested with about 90 indentations along the center line of the sheets' cross section. Some of the specimens that were used for the micro-hardness testing were subsequently etched in a solution of 2% HNO_3 to reveal the microstructure by light optical microscopy (Leica DM 400).

4. Results and Discussion

4.1 Cooling Rates and Holding Temperatures

A typical temperature profile for the entire process is depicted in Fig. 6. Extraction of the hot sheets from the furnace, transfer in a thermally insulated container and placing them onto the temperature control plate takes about 10 s. Thus, the sheet temperature when starting the pre-cooling by compressed air is in the range of 970–1000 °C. After the first 10 s of air cooling, the temperature drops down to 700 °C for a pressure of 0.1 MPa and to about 520 °C at 0.4 MPa. The greater the air pressure, the lower the difference between the cooling curves at the different pressures. The end temperature after this cooling stage in the center of the pre-cooled zone (point 3 in Fig. 2) ranged from 330 to 505 °C, and thus mean cooling rates were between 12 to 16 K/s (s. Table 5). Transferring the sheets for water quenching took 5-7 s, and from Fig. 6 the temperature increase is about 80-90 °C with reheating rates of 12–16 K/s. This reheating is caused by the heat transfer from the inside of the sheets towards the surface as well as from the non-cooled material areas to those which were pre-cooled.

4.2 Mechanical Properties

The tensile test results of a set of specimens taken from softened air pre-cooled zones are summarized in Table 6. The differences in the ultimate tensile strength of samples cooled at air pressures of 0.2 MPa and above are marginal. The yield strength is more sensitive to the air pressure: it changes from approx. 700 MPa for samples treated with 0.1 MPa up to about 900 MPa with 0.4 MPa. This is in accordance with data of (Ref 31) where the authors obtained tensile strength values of 800 MPa (cooling rate not specified). In another work, Güler et al. (Ref 32) reported tensile strength values of 757 MPa for sheets with a thickness of 1.7 mm after cooling from 950 °C in still air.

Though decreasing values of total elongation at fracture with increasing air pressure were observed, the values of the total elongation are not given in Table 6 since the tensile specimens featured a non-homogenous microstructure distribution and the chosen test geometry did not conform to the standard. Instead, the Vickers hardness was measured across the pre-cooled zones.

4.3 Microstructure and Hardness Distribution Upon Pre-cooling with 0.1 MPa

The typical distribution of the hardness in the pre-cooled area is depicted in Fig. 7 (cooling time 40 s; tube-to-sheet distance 5 mm). The upper green line gives reference values of the non-pre-cooled sheet section with values of about 500 HV5. As intended, a significant hardness reduction in the pre-cooled zones could be realized; the hardness data show a good reproducibility for different samples. With values of 250-300 HV5, the Vickers hardness in the softened zone corresponds to
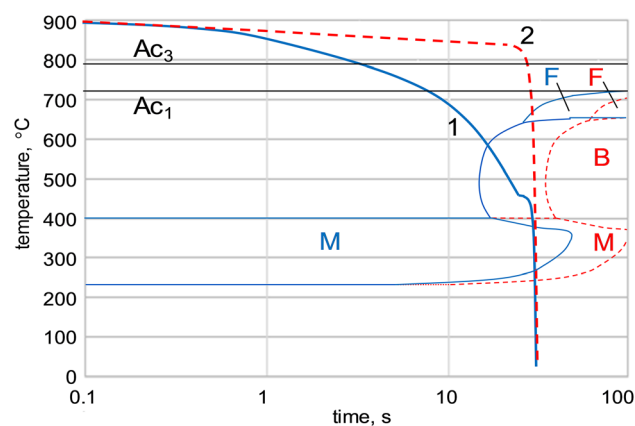

Fig. 5 Time–temperature–transformation (TTT) diagram and proposed cooling regime in "soft" (1) and "hard" (2) zones

Table 4 Cooling conditions used in the experiments

| | | | Air pre-cooling | | | | | | |
| | | | Initial step | | | Second step | | | |
#	Nozzle type*	Cooling distance, mm	Air pressure, MPa	Flow rate, l/min	Duration, s	Air pressure, MPa	Flow rate, l/min	Duration, s	Type of final cooling
1	IT	5	0.1	58	40	–	–	–	Water bath
2	IT	5	0.2	94	40	–	–	–	
3	IT	5	0.3	129	40	–	–	–	
4	IT	5	0.4	164	40	–	–	–	
5	IT	10	0.2	94	40	–	–	–	
6	IT	20	0.2	94	40	–	–	–	
7	IT	10	0.2	94	30	–	–	–	
8	IT	10	0.05	38	10	0.1	58	10	
9	IT	10	0.05	38	15	0.1	58	10	
10	IT	10	0.05	38	15	0.1	58	15	
11	IT	10	0.05	38	15	0.1	58	10	Water cooled tool
12	IT	10	0.05	38	15	0.1	58	15	
13	PJ	10	0.05	38	15	0.1	58	10	
14	PJ	10	0.05	38	15	0.1	58	15	

* IT: inner tube, PJ: small point jet nozzle

a bainitic microstructure. The diameter of the softened zone is slightly greater than the inner diameter of the outer tube. This can be explained by two effects: heat transfer between pre-cooled and untreated zones and heat transfer due to direct contact with the outer exhaust tube (steel tube with wall thickness 1.8 mm).

The microstructures in the key areas featuring the different hardness values are displayed in Fig. 8. The non-pre-cooled sheet sections from the center of the blank (pos. "d" in Fig. 7) show a fully martensitic microstructure (brown). Areas with the lowest hardness (pos. "a") and in the center of pre-cooled zone (pos. "b") are bainitic (grey) with only small fractions of martensite. The transition area (pos. "c") is characterized by a mixed microstructure and hardness values of 400 HV5 where the amount of martensite is in excess of bainite and pearlite (black).

4.4 Microstructure and Hardness Distribution for Increased Air Pressures During Pre-cooling

Application of air pressures of more than 0.1 MPa resulted in a convex form of the hardness profile (cf. Fig. 9). At pressures of 0.3 MPa and 0.4 MPa, this convexity transforms to a plateau reaching levels of 435 HV5 and 440 HV5, respectively. The higher the pressure, the smaller the deviation of hardness values between different samples (about ± 10 HV5 for pressures of 0.3 and 0.4 MPa). The mean hardness values are given in Table 7. Remarkably, the zone with minimal hardness (260–270 HV5) grows in diameter from 17 to 36 mm (±2 mm) with increasing air pressures. It can be assumed that this softened annular-shaped section of the material is caused due to heat conduction between the pre-cooled and the non-pre-cooled sheet areas. This effect can be exploited in case the

Fig. 6 Time-temperature profiles for varied air pressures (reference—center of blank without cooling; cooling distance tube-to-sheet 5 mm, cooling time 40 s—experiments no. 1–4 in Table 4)
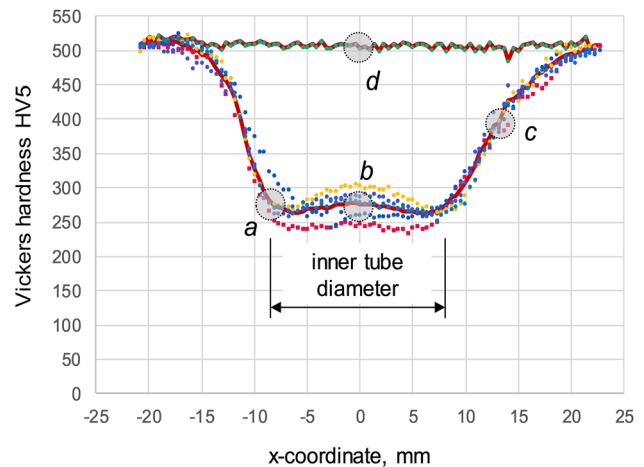

Fig. 7 Hardness profile in pre-cooled zones and for non-pre-cooled reference positions (upper green line); mean values of five different samples (experiment no. 1 in Table 4). The corresponding microstructures at positions "a" to "d" are depicted in Fig. 8

Table 5 Influence of the air pressure on the temperature in the center of the pre-cooling zone at the end of the pre-cooling with compressed air

Air pressure, MPa	Temperature*, °C	Mean cooling rate during pre-cooling, K/s	Cooling rate (800–500 °C), K/s
0.1	505	12.0	9.1
0.2	430	13.7	19.6
0.3	345	15.9	25.4
0.4	330	16.3	27.3
* when cooling from 980 °C			

Table 6 Mechanical properties of the tensile samples with pre-cooled soft zone (cooling time 40 s, tube-to-sheet distance 5 mm)

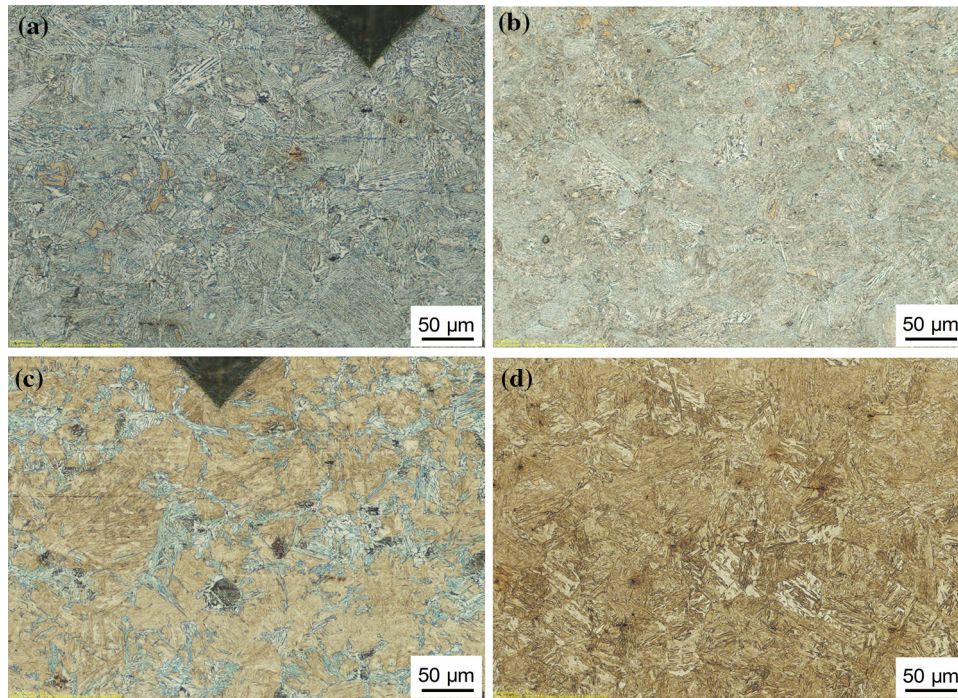| Air pressure, MPa	Ultimate tensile strength, MPa	0.2% offset yield stress, MPa
0.1	855	694
0.2	890	756
0.3	902	852
0.4	904	887

Fig. 8 Microstructure in different areas of the locally pre-cooled blank of experiment no. 1 from Table 4: a—area with lowest hardness (pos. "*a*" in Fig. 7), b—area in the center of the air cooled zone (pos. "*b*" in Fig. 7), c—transition area (pos. "*c*" in Fig. 7), d—non-pre-cooled center of the blank (pos. "4" in Fig. 2 and pos. "*d*" in Fig. 7); martensite—brown, bainite—grey, pearlite—black
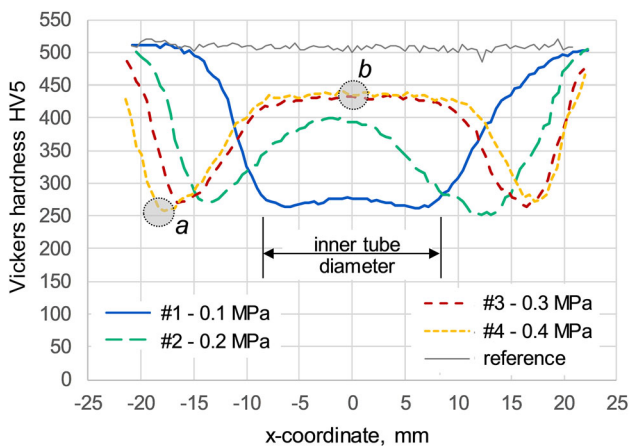

Fig. 9 Hardness profiles across the pre-cooled softened zones after cooling at different air pressures (experiments no. 1–4 in Table 4, reference—center of the blank without pre-cooling). The microstructures in areas marked "*a*" and "*b*" are depicted in Fig. 10

treated zones are to be punched-out later. The diameter of the softened circular zone can be varied easily by changing the air pressures without modifying the feeding and tubular cooling device. The small changes of the minimal hardness are reflected in the moderate variations of tensile strength (up to 6%) for different air pressure levels (cf. Table 6).

The width of the transition zone between soft and fully hardened material sections is not sensitive to the air cooling parameters and ranges from 5 mm to 10 mm, which is significantly lower than reported (Feu16, Hie16). This value also depends on the contact conditions between the tabular

cooling device and the treated blank. Thus, it appears reasonable to assume that the diameter of the pre-cooled zone could be decreased further.

The microstructure of a specimen pre-cooled at an air pressure of 0.4 MPa shows a mostly bainitic microstructure (Fig. 10a) in the area of minimal hardness (pos. "*a*" in Fig. 9), while martensite dominates in the central area (pos. "*b*," Fig. 9).

4.5 Influence of Tube-to-Sheet Distance and Duration of Pre-cooling

Increasing the tube-to-sheet distance has no pronounced influence on the hardness values (Fig. 11). The maximum difference in the center for samples pre-cooled with a distance of 5 and 20 mm was only to 30 HV5; with decreasing distance, the hardness in the center increases.

Decreasing of the pre-cooling time from 40 to 30 s (Fig. 11) results in an increase in the minimal hardness of about 20 HV5, while the diameter of circular softened area drops from 28 to 23 mm. Hence, decreasing the cooling time is another parameter to control the size of a softened zone. In addition, this provides an opportunity to decrease the total cooling time.

4.6 Two-Step Pre-cooling

In the second set of the experiments, a two-step cooling setup was used with a flow rate in the first phase of 38 and 58 l/min in the second. The time of each phase was set to 10 or 15 s (no. 8–10 in Table 4). The hardness distributions in the pre-cooled areas for three different parameter combinations are depicted in Fig. 12. It is apparent that the shortest pre-cooling time of 20 s results in the highest observed hardness level of

Table 7 Effect of air pressure used in pre-cooling on hardness values and diameter of the zones from Fig. 9

Air pressure, MPa	Hardness in the pre-cooled center, HV5	Diameter of the plateau, mm	Minimal value of hardness, HV5	Diameter of minimum value hardness zone, mm	Diameter of cooling affected zone, mm
0.1	275	17	260	17	35
0.2	400	…	265	26	41
0.3	435	15	270	33	44
0.4	440	17	270	36	46
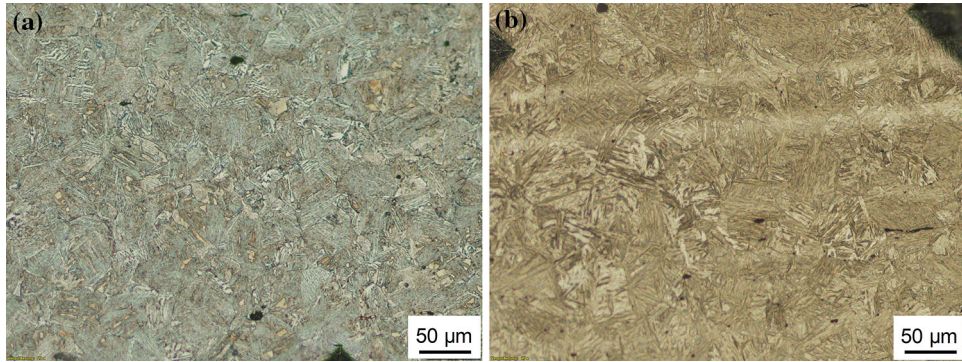
Fig. 10 Microstructure in different areas of the pre-cooled and quenched blank, experiment no. 4 from Table 4: a—zone with minimal hardness (pos. "*a*" in Fig.9), b—zone in the center of pre-cooled area (pos. "*b*" in Fig. 9); martensite—brown, bainite—grey, pearlite—black
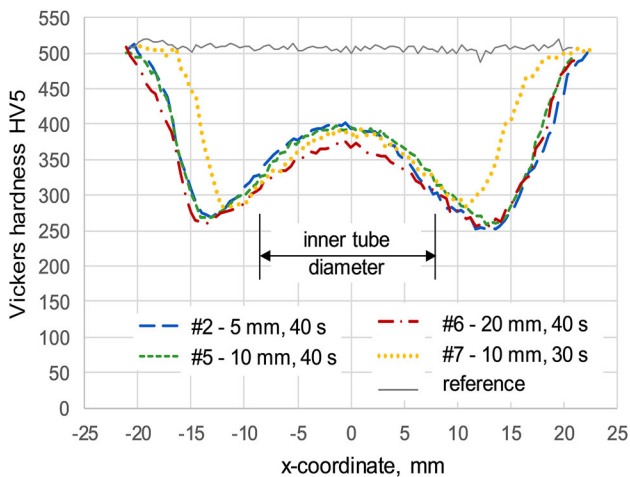
Fig. 11 Hardness profiles in pre-cooled softened zones after cooling at air pressures of 0.2 MPa and varied tube-to-sheet distances and times of cooling, experiments no. 2, 5–7 in Table 4 (reference—center of blank, without pre-cooling)

Fig. 12 Hardness profiles after two-step inner tube air pre-cooling with a final quenching in a water bath—experiments no. 8–10 in Table 4

about 350 HV5, whereas at 25 and 30 s a hardness of 300 HV5 was obtained in the center. Moreover, the soft zone after a treatment of 30 s is broadened.

4.7 Integration of Pre-cooling into a Hot Stamping Process

The results obtained for processing pre-cooled blanks by hot stamping with water cooled dies instead of water quenching are depicted in Fig. 13 for the tubular cooling and an alternative cooling where an additional point jet nozzle (PJ) was mounted on the inner tube. As expected, the reference hardness of 470 HV5 is somewhat lower as compared to the reference hardness
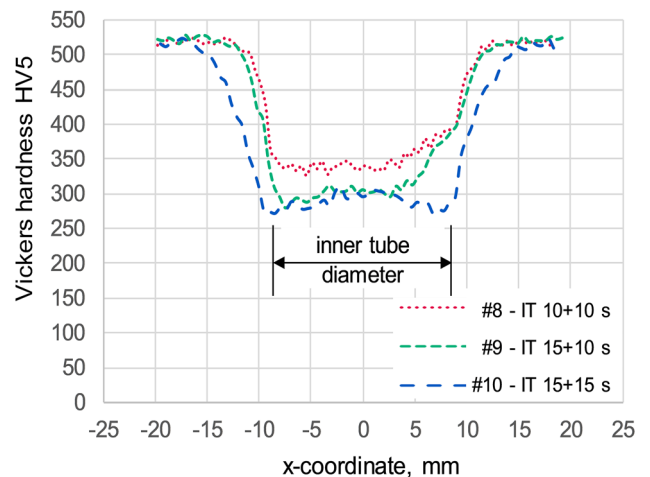
of 500 HV5 determined for water quenched sheets. Similar to the observations made when water quenching, a process of 30 s has a slight tendency toward forming a convex HV-curve in the center as compared to a process of 25 s. With a diameter of 25 mm, the softened zone is even more pronounced than the one obtained by water quenching.

The lowest hardness level of approximately 260 HV5 was achieved by the application of a small point jet nozzle as the closing of the inner tube. The diameter of the hardness plateau is approximately 14 mm, while the overall diameters of the affected zones are 26 and 34 mm for cooling times of 25 and 30 s, respectively. Hence, the application of small point jet
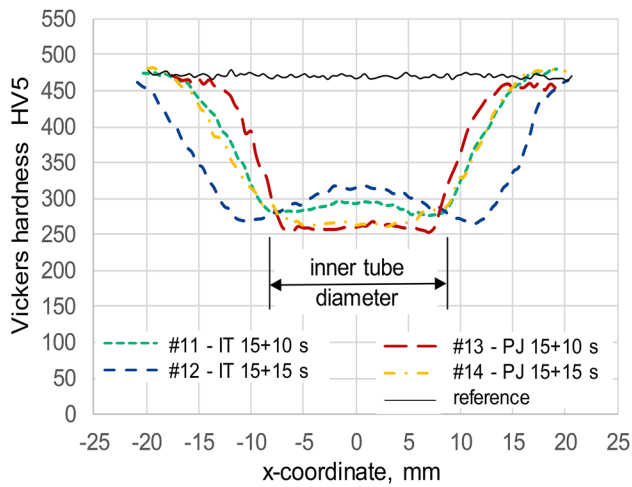
Fig. 13 Hardness profiles after a two-step air pre-cooling and hot stamping—experiments no. 11–14 in Table 4: IT—application of inner tube pre-cooling; PJ—application of a point jet nozzle; reference—non-pre-cooled material

nozzles allows providing a constant low level of hardness during hot stamping, which can be varied easily by adapting the cooling time.

5. Summary and Conclusions

In order to obtain soft local zones suited for mechanical joining after hot stamping, a multi-step cooling process is proposed. In the first stage—while the main blank remains austenitized—the later soft local zones are pre-cooled by compressed air prior to the actual hot stamping in order to obtain a bainitic microstructure. Subsequently, hot stamping can be carried out to generate a martensitic microstructure in the not pre-cooled material sections. To realize the process, a tubular air-cooling device was designed in combination with a sheet insulation containment while applying the local pre-cooling with compressed air.

Varying the air pressure during pre-cooling in the range from 0.1 to 0.4 MPa resulted in a temperature in the center of cooling between 505 and 330 °C. A pre-cooling treatment at 0.1 MPa air pressure for 40 s allowed obtaining a significantly softened bainitic zone (260–270 HV5) with a diameter approximately equal to the diameter of the outer exhaust tube. The hardness of the material outside the pre-cooled sections was unaffected with constant values of about 500 HV5. Increasing the air pressure up to 0.4 MPa increased the diameter of the zone with a minimal hardness from 17 to 36 mm, while the hardness in the center of the pre-cooled zone was up to 440 HV5. The transition zone between soft and hardened had a length of 5-10 mm. Increasing the tube-to-sheet distance from 5 to 20 mm let to only marginal growth of hardness by about 30 HV5. Changing the air cooling time from 40 to 30 s resulted in a slight increase in minimal hardness by $\approx$ 20 HV5, but the diameter of the circular soft zone dropped by 18%. Modification of the tubular cooling device and application of a two-stage cooling with an initial air pressure of 0.05 MPa and a subsequent pressure of 0.1 MPa allowed

decreasing the cooling time to 20-25 s with a resulting hardness level in the softened zone of approximately 300 HV5.

Trials with an industrial press demonstrated that the approach can applied to industry relevant conditions. In this case, pre-cooling followed by hot stamping with a water cooled tool resulted in lowest hardness of about 260 HV5, which is also substantial decrease as compared to the hardness value of 470 H5 determined for the non-pre-cooled sections of the material. The size of the soft zone and cooling-affected zone can be varied by changing the air pressure and the cooling time without modification of the presented tubular air-cooling device.

The proposed process chain with pre-cooling prior when hot stamping to obtain soft local zones allows to use conventional furnaces and hot stamping tools. In addition, it does not contribute to distortion of the final parts as the process is applied prior to hot-stamping. The considered type of air-cooling devices can be integrated into production lines and used in parallel in order to provide a high productivity. Application of air pre-cooling instead of water-air spray cooling allows to avoid vapor formation as well as issues with oxidation of the treated zones.

References

1. H. Karbasian and A.E. Tekkaya, A Review on Hot Stamping, *J. Mater. Process. Technol.*, 2010, **210**, p 2103–2118
2. C. Löbe, O. Hering, L. Hiegemann, and E. Tekkaya, Setting Mechanical properties of High Strength Steels for Rapid Hot Forming Processes, *Materials*, 2016, **9**, p 229. https://doi.org/10.3390/ma9040 229
3. K. Mori, B.F. Bariani, B.-A. Behrens, A. Brosius, M. Merklein, and J. Yanagimoto, Hot Stamping of Ultra-High Strength Steel Parts, *CIRP Ann.*, 2017, **66**(2), p 755–777
4. Tailored Tempering (Tailored Tempering), Digital Engineering Magazine, 2014, 02, p 24–25 **(in German)**

5. J. Shi, in *Investigation of the Effects of Heating and Quenching on the Mechanical Properties and Microstructure of 22MnB5 Steel Sheets*, 2018, Electronic Theses and Dissertations, 7444. https://scholar.uwindsor.ca/etd/7444

6. B.-A. Behrens, C.M. Gaebel, J. Moritz, and J. Schrödter, Hot Stamping of Load Adjusted Structural Parts, *Proc. Eng.*, 2014, **81**, p 1756–1761

7. M. Glatzer, T. Stöhr, M. Merklein, S. Sikora, K. Lamprecht, G. Deinzer, Einfluss unterschiedlicher Wärmebehandlungsrouten auf die Robustheit der mechanischen Eigenschaften des Stahls 22MnB5 (Influence of different heat treatment routes onto robustness of mechanical properties of steel 22MnB5) 4, in *Erlanger Workshop Warmblechumformung, DFG ortsverteilte Forschergruppe 552, 11. Nov, 2009, (Erlangen, DE)*, (Meisenbach), p. 85–105 **(in German)**

8. F.-J. Lenze, J. Banik, S. Sikora, T. Gerber, Further development of manganese boron steels for the lightweight design of body in white structures, in *IDDRG: International Deep Drawing Research Group Conference, Tools and Technologies for the Processing of Ultra High Strength Steels, Conf Proc*, May 31–Jun 2, 2010 (Graz, AT), (TU Graz), p. 17–26

9. L.O. Wolf, F. Nürnberger, D. Rodman, and H.J. Maier, 1-Step "Quenching and Partitioning" of the Press-Hardening Steel 22MnB5, *Steel Res. Int.*, 2017, **88**(6), p 1600307

10. L.O. Wolf, J.-P. Cordebois, D. Rodman, F. Nürnberger, and H.J. Maier, Effect of Different Intercritical Annealing Treatments Without and With Overaging on the Mechanical Material Behavior, *Steel Res. Int.*, 2018, **89**(10), p 1800196

11. L.O. Wolf, F. Nürnberger, D. Rodman, and H.J. Maier, The Effect of Intercritical Annealing on the Microstructure and Mechanical Properties of Ferritic-Martensitic Two-Phase Steels, *Steel Res. Int.*, 2017, **88**(2), p 271–280

12. M. Maikranz-Valentin, U. Weidig, U. Schoof, H.-H. Becker, and K. Steinhoff, Components with Optimised Properties due to Advanced Thermo-Mechanical Process Strategies in Hot Sheet Metal Forming, *Steel Res. Int.*, 2008, **79**(2), p 92–97

13. T. Stöhr, J. Lechler, M. Merklein, Investigations on different strategies for influencing the microstructural properties with respect to partial hot stamping, in *2nd International Conference on Hot Sheet Metal Forming of High-Performance Steel*, Jun 15–17, 2009 (Lulea, SE) (Verlag Wissenschaftliche Scripten), p. 273–281

14. B.-A. Behrens, A. Chugreev, M. Jalanesh, K. Wölki, F. Bohne, Parametrisation of a numerical model for a partial heating strategy used to evaluate a masking concept of a hot stamping process, Metal 2019, in *28th International Conference of Metallurgy and Materials*, p. 320–325

15. M. Merklein, J. Lechler, and T. Stoehr, Investigations on the Thermal Behavior of Ultra High Strength Boron Manganese Steels Within Hot Stamping, *Int. J. Mater. Form.*, 2009, **2**(259), p 259–262

16. F. Zimmermann, W. Volk, J. Spörer, M. Pfestorf, Aktuelle Anwendungen im Bereich der Warmumformung höchstfester Stahlgüten im Karosseriebau und zukünftige Trends (Actual applications in the field of hot deformation of high strength steel products in the car body construction and future trends). 6. Erlanger Workshop Warmblechumformung, DFG ortsverteilte Forschergruppe 552, 17. Nov, 2011 (Erlangen, DE), Meisenbach, p. 81–94 **(in German)**

17. T. Marten, J. Niewel, and T. Tröster, Investigation on Alternative Heating Concepts for the Hot Sheet Metal Forming, *HTM*, 2011, **66**, p 309–315

18. W. Liang, L. Wang, Y. Liu, Y. Wang, and Y. Zhang, Hot Stamping Parts with Tailored Properties by Local Resistance Heating, *Procedia Eng.*, 2014, **81**, p 1731–1736

19. A. Andreiev, O. Grydin, and M. Schaper, Evolution of Microstructure and Properties of Steel 22MnB5 Due to Short Austenitization with Subsequent Quenching, *Steel Res. Int.*, 2016, **87**(12), p 1733–1741

20. M.J. Holzweissig, J. Lackmann, S. Konrad, M. Schaper, and T. Niendorf, Influence of Short Austenitization Treatments on the Mechanical Properties of Low-Alloy Steels for Hot Forming Applications, *Metall. Mater. Trans. A*, 2015, **46**, p 3199–3207

21. O. Grydin, A. Andreiev, M.J. Holzweißig, C.J. Rüsing, K. Duschik, Y. Frolov, and M. Schaper, Shot Austenitization Treatment with Subsequent Press Hardening: Correlation Between Prozess Parameters, Microstructure and Mechanical Properties, *Mater. Sci. Eng., A*, 2019, **749**, p 176–195

22. C. Hielscher, S. Horn, Werneke, C. Buse, Herstellung von gradierten Bauteileigenschaften beim Presshärten durch gezielte Zwischenkühlung, 11. Erlanger Workshop Warmblechumformung, 17 Nov, 2016 (Erlangen, DE), Meisenbach, p. 77–92 **(in German)**

23. H. Lehmann, P. Feuser, Realisierung von "Tailored Properties" an pressgehärteten Bauteilen mittels "Thermischem Printing", 11. Erlanger Workshop Warmblechumformung, 17 Nov, 2016 (Erlangen, DE), Meisenbach, p. 63–75 **(in German)**

24. M. Merklein, M. Wieland, M. Lechner, S. Bruschi, and A. Ghiotti, Hot Stamping of Boron Steel Sheets with Tailored Properties: A Review, *J. Mater. Process. Technol.*, 2016, **228**, p 11–24

25. L. Galdos, E. Sanz de Argandona, R. Ortubay, Towards the Generation of Taylored Tempered Components: Concept Definition and Process Parameters Optimization, in *IDDRG: International Deep Drawing Research Group Conf., June 2 - 5, 2013 (Zurich, Switzerland) Conf. Proc. CD ROM, Institute of Virtual Manufacturing* (ETH Zurich), p. 425–430

26. M. Diekamp, S. Hübner, F. Nürnberger, M. Schaper, B.-A. Behrens, and F.-W. Bach, Prozessoptimiertes Presshärten Mittels Sprühkühlung—Prozessintegrierte Wärmebehandlung von Blechen des Werkstoffes 22MnB5, *HTM J. Heat Treat. Mater.*, 2011, **6**, p 316–322

27. F. Nürnberger, M. Diekamp, J. Moritz, L. Wolf, S. Hübner, B.-A. Behrens, Spray Cooling of Early Extracted Hot Stamped Parts, in TMS2014 Annual Meeting Supplemental Proc., Annual Meeting; 143rd, Minerals, Metals and Materials Society, 2014 (San Diego, CA) (Wiley, New York) p. 983–990

28. M. Merklein, T. Stöhr, T. Svec, M. Wieland, Funktionsoptimierte Strukturbauteile im Presshärtprozess (Functional Optimized Structural Componenets in Press Hardening), Lightweight Design, 2010, 3(5), Vieweg+Teubner Verlag, pp. 52–58

29. M. Spittel, T. Spittel, SpringerMaterials, Steel symbol/number: 22MnB5/1.5528, Landolt-Börnstein - Group VIII Advanced Materials and Technologies 2C1, 2009. https://materials.springer.com/lb/docs/sm_lbs_978-3-540-44760-3_146

30. M. Naderi, L. Durrenberger, A. Molinari, and W. Bleck, Constitutive Relationship for 22MnB5 Boron Steel Deformed Isothermally at High Temperatures, *Mater. Sci. Eng.*, 2008, **478**, p 130–139

31. H. Liu, J. Yu, and H. Zhao, Microstructure and Mechanical Properties of 22MnB5 Steel with Different cooling Method, *Appl. Mech. Mater.*, 2013, **331**, p 555–558

32. H. Güler, R. Ertan, and R. Özcan, Influence of Heat Treatment Parameters on the Microstructure and Mechanical Properties of Boron-Alloyed Steels, *Mater. Test.*, 2012, **54**(9), p 619–624

Publisher's Note Springer Nature remains neutral with regard to jurisdictional claims in published maps and institutional affiliations.